

## Small effects in sub-barrier heavy-ion elastic scattering

M. S. Hussein, V. L. M. Franzin, and R. Franzin

*Instituto de Física, Universidade de São Paulo, São Paulo, SP, Brazil*

A. J. Baltz

*Physics Department, Brookhaven National Laboratory, Upton, New York 11973*

(Received 29 December 1983)

The effects of virtual Coulomb excitation of giant multipole resonances as well as of relativity on sub-barrier elastic scattering of heavy ions are investigated. Closed expressions for the effect of giant quadrupole and octopole excitation from the adiabatic polarization potential, on the elastic scattering differential cross section, are derived. Comparison with optical model and coupled channels calculations is reported. The effect of special relativity on the Rutherford cross section is also described in a closed form.

### I. INTRODUCTION

The predominant feature of sub-barrier heavy-ion elastic scattering is the point Coulomb repulsion. However, it is quite well known that deviations from this pure Rutherford scattering do arise as a consequence of Coulomb excitation of nuclear collective states. These excitation processes are of a long-range nature and thus occur at distances equal to or larger than the Coulomb distance of closest approach.

Recent measurements<sup>1</sup> of angular distributions of elastically scattered light heavy projectiles from deformed target nuclei have clearly exhibited these deviations in the form of a long-range absorption arising from the strong Coulomb excitation of low-lying collective states. Aside from these deviations, other, albeit smaller, ones occur as a result of several factors. The excitations of the high-lying collective giant multipole resonances, atomic screening, relativistic corrections, and vacuum polarization are usually cited in this connection.<sup>2</sup>

Owing to the smallness of these latter deviations ( $\sim 1.0\%$ ) their clear identification is a challenge to experimentalists. Recently, Lynch *et al.*<sup>3</sup> have presented a clear evidence of these effects in the sub-barrier elastic scattering of closed-shell heavy-ion systems, where Coulomb excitations of low-lying collective states are negligible.

Prior to these measurements several theorists have calculated numerically the deviations arising from the excitation of the giant dipole resonance, relativistic effects, as well as atomic screening. Baur *et al.*<sup>4</sup> have derived, within first-order classical perturbation theory, a closed expression for the deviation from Rutherford scattering due to virtual excitation of the giant dipole.

The purpose of the present paper is to extend the calculation of Ref. 4 to include the Coulomb excitation of giant quadrupole and octopole resonances as well as the relativistic corrections. Furthermore, a careful verification of the validity of the classical calculation is provided through comparison with coupled channels calculations.

The paper is organized as follows. In Sec. II a detailed discussion of the adiabatic polarization potential arising

from the Coulomb couplings to giant multipole resonances is given. In Sec. III the relativistic corrections are carefully analyzed. Closed form expressions for the corresponding deviations from the point Coulomb (Rutherford) scattering, are presented in Sec. IV. Comparison with coupled channels (CC) calculations, and the resulting trivially equivalent local polarization potentials, is then given in Sec. V. Concluding remarks and a discussion are the subject of Sec. VI. A brief summary account of some of our results has been presented previously (Ref. 5).

### II. ADIABATIC GIANT MULTIPOLE POLARIZATION POTENTIALS

The amplitude for the excitation of a vibrational state of multipolarity  $\lambda$ , and excitation energy  $\Delta E_\lambda$ , using the first-order time-dependent theory of Coulomb excitation, is given by

$$a_\lambda(\infty) = \frac{1}{i\hbar} \int_{-\infty}^{\infty} \langle n | V(r(t)) | 0 \rangle e^{i\Delta E_\lambda t / \hbar} dt. \quad (1)$$

The interaction  $V(r(t))$  has a matrix element  $\langle n | V(r) | 0 \rangle$  proportional to  $[r(t)]^{-\lambda-1}$ . We therefore have for  $a_\lambda(\infty)$

$$a_\lambda(\infty) = C \int_{-\infty}^{\infty} \frac{\exp(i\Delta E_\lambda t / \hbar)}{[r(t)]^{\lambda+1}} dt, \quad (2)$$

where  $C$  is a constant. The largest contribution to the integral in Eq. (2) comes from the vicinity of the classical turning point,  $r_{\text{tp}} \equiv r(0)$ . Thus by expanding

$$r(t) \simeq r_{\text{tp}} + \frac{1}{2} \ddot{r}_{\text{tp}} t^2,$$

and keeping lowest order terms in  $t$ , one obtains the simple estimate

$$a_\lambda(\infty) = C \frac{\pi}{r_{\text{tp}}^{\lambda+1}} \left[ \frac{2r_{\text{tp}}}{(\lambda+1)\ddot{r}_{\text{tp}}} \right]^{1/2} \times \exp \left\{ - \left[ \frac{2r_{\text{tp}}}{(\lambda+1)\ddot{r}_{\text{tp}}} \right]^{1/2} \omega_\lambda \right\}, \quad (3)$$

where  $\ddot{r}_{\text{tp}}$  is the radial acceleration at the classical turning point and  $\omega_\lambda \equiv \Delta E_\lambda / \hbar$ . Introducing the average collision time  $\tau_{\text{coll}} \equiv (r_{\text{tp}} / \dot{r}_{\text{tp}})^{1/2}$ , we have finally

$$a_\lambda(\infty) = C \frac{\pi}{r_{\text{tp}}^{\lambda+1}} \left[ \frac{2}{\lambda+2} \right]^{1/2} \tau_{\text{coll}} \times \exp \left[ - \left[ \frac{2}{\lambda+1} \right]^{1/2} \omega_\lambda \tau_{\text{coll}} \right] \quad (4a)$$

$$= C \frac{\pi}{r_{\text{tp}}^{\lambda+1}} \left[ \frac{2}{\lambda+1} \right]^{1/2} \tau_{\text{coll}} \times \exp \left[ -2 \left[ \frac{1}{\lambda+1} \right]^{1/2} \frac{\Delta E}{E_{\text{c.m.}}} \eta \right], \quad (4b)$$

where  $\eta$  is the Sommerfeld parameter,  $\eta = Z_p Z_T e^2 / \hbar v$ ,  $v$  being the asymptotic relative velocity.

For heavy ion scattering at low energies  $\eta \gg 1$ , therefore, one expects

$$\omega_\lambda \tau_{\text{coll}} \equiv \sqrt{2} \frac{\Delta E_\lambda}{E_{\text{c.m.}}} \eta$$

to be much larger than unity for the excitation of high-lying collective states [giant resonances (GR)]. This indicates that  $a_\lambda^{\text{GR}}(\infty) \ll 1$ ; accordingly, very little amount of flux is lost from the elastic channel. On the other hand,  $a_\lambda(\infty) \simeq 1$  for the excitation of low-lying collective states, which reflects the need to incorporate into the elastic channel optical potential the resulting absorptive long-range component.

As a consequence of the smallness of  $a_\lambda^{\text{GR}}(\infty)$  at sub-barrier energies, one expects that the polarization potentials obtained from, e.g., coupled channels calculation, to be predominantly real. This is borne out by actual CC calculations (see discussion to follow).

The adiabatic polarization potential of multipolarity  $\lambda$  was derived 28 years ago by Alder *et al.*<sup>6</sup> using second-order perturbation theory. The result is

$$V_{\text{ad pol}}^{(\lambda)}(r) = \left[ 4\pi Z_p^2 e^2 \frac{1}{(2\lambda+1)^2} \times \sum_{n \neq 0} \frac{B(E\lambda; 0 \rightarrow n)}{E_0 - E_n} \right] / r^{2\lambda+2}. \quad (5)$$

We can estimate the strength of  $V_{\text{ad pol}}^{(\lambda)}(r)$  by the use of the energy-weighted sum rule. This is accomplished by writing

$$\begin{aligned} \sum_{n \neq i} \frac{B(E\lambda; 0 \rightarrow n)}{E_0 - E_n} &= \sum_{n \neq 0} \frac{B(E\lambda; 0 \rightarrow n)(E_0 - E_n)}{(E_0 - E_n)^2} \\ &\simeq \frac{-1}{(\Delta E_\lambda)^2} \sum_n B(E\lambda; 0 \rightarrow n)(E_n - E_0) \\ &\equiv -\frac{S(E\lambda)}{(\Delta E_\lambda)^2}, \end{aligned} \quad (6)$$

where we have introduced the familiar notation for the energy weighted sum rule<sup>7</sup>

$$S(E\lambda) = \sum_n B(E\lambda; 0 \rightarrow n)(E_n - E_0) \quad (7)$$

and denoted the excitation energy of the  $\lambda$ -pole giant resonance by  $\Delta E_\lambda$ .

Bohr and Mottelson<sup>7</sup> derived a classical model-independent expression for  $S(E\lambda)$ , which we write below

$$\begin{aligned} S(E1) &= 14.8 \frac{NZ}{A} (e^2 \text{ fm}^2 \text{ MeV}), \\ S(E\lambda) &= \frac{3\lambda(2\lambda+1)}{4\pi} \frac{\hbar^2}{2m} \frac{Z^2}{A} \\ &\quad \times (R)^{2\lambda-2} (e^2 \text{ fm}^{2\lambda} \text{ MeV}), \quad \lambda \geq 2 \end{aligned} \quad (8)$$

where  $N$  is the neutron number,  $m$  is the mass of the nucleon, and  $R$  is the radius of the nucleus.

In terms of  $S(E\lambda)$  and  $\Delta E_\lambda$ , our adiabatic polarization potential, Eq. (5), may now be written as [after allowing for the mutual excitation of both target ( $T$ ) and projectile ( $p$ )]

$$\begin{aligned} V_{\text{ad pol}}^{(\lambda)}(r) &= -\frac{4\pi e^2}{(2\lambda+1)^2} \left[ \frac{Z_p^2 S_T(E\lambda)}{(\Delta E_\lambda(T))^2} + \frac{Z_T^2 S_p(E\lambda)}{(\Delta E_\lambda(p))^2} \right] \\ &\quad \times r^{-2\lambda-2} (\text{MeV}). \end{aligned} \quad (9)$$

Clearly the above expression for  $V_{\text{ad pol}}^{(\lambda)}(r)$  should be used in the discussion of heavy-ion elastic scattering at sub-barrier energies. At center-of-mass energies above the barrier the above form should be considered valid for  $r > R_c$ , where  $R_c$  is the radius of the charge distribution. At separation distances smaller than  $R_c$ , the form of  $V_{\text{ad pol}}^{(\lambda)}(r)$  becomes

$$\begin{aligned} V_{\text{ad pol}}^{(\lambda)}(r) &= \left[ \frac{\lambda+1}{\lambda+2} \right]^2 V_{\text{ad pol}}^{(\lambda)}(R_c) \\ &\quad \times \left[ \frac{2\lambda+3}{\lambda+1} - \left[ \frac{r}{R_c} \right]^{\lambda+2} \right]^2, \end{aligned} \quad (10)$$

where  $V_{\text{ad pol}}^{(\lambda)}(R_c)$  is given by Eq. (9).

In our discussion to follow we consider sub-barrier elastic scattering only, and therefore Eq. (9) suffices. To get a feeling about the magnitude of the effect, we give, below, general expressions for the isovector giant dipole ( $\lambda=1, T=1$ ) resonance component and the isoscalar giant quadrupole resonance ( $\lambda=2, T=0$ ) component of  $V_{\text{ad pol}}(r)$  (Ref. 8)

$$\begin{aligned} V_{\text{ad pol}}^{(1)}(r) &= -6.7 \times 10^{-3} \left[ \frac{N_p}{Z_p A_p^{1/3}} + \frac{N_T}{Z_T A_T^{1/3}} \right] \\ &\quad \times Z_p^2 Z_T^2 / r^4 (\text{MeV}), \\ V_{\text{ad pol}}^{(2)T=0}(r) &= -0.0208 (A_p^{1/3} + A_T^{1/3}) \\ &\quad \times Z_p^2 Z_T^2 / r^6 (\text{MeV}). \end{aligned} \quad (11)$$

The above expressions were obtained by inserting the expressions for  $S(E\lambda)$ , Eq. (8), into Eq. (9) and using for the radius parameter ( $R = r_0 A^{1/3}$  fm) the electron scattering value  $r_0 = 1.2$  fm. For the excitation energies  $\Delta E_{\lambda=1}$  and  $\Delta E_{\lambda=2}$ , we have used the empirical values  $80.0 A^{-1/3}$

MeV and  $60/0A^{-1/3}$  MeV, respectively. For nuclei with masses  $A < 40$ , the expression of  $\Delta E_{\lambda=1}$  given above is not valid and one should instead use the following:

$$\Delta E_{\lambda=1} \simeq \frac{64 \cdot 65}{A^{1/3}} - \frac{17 \cdot 4}{A^{2/3}} \text{ (MeV)}, \quad (12)$$

which follows reasonably well the systematics of the giant dipole resonance energies of light nuclei ( $A < 40$ ).

Finally, one may easily add the contribution of the isovector giant quadrupole resonance to  $V_{\text{ad pol}}^{(2)}(r)$  of Eq. (11b), by recognizing that the excitation energy of the ( $\lambda=2, T=1$ ) resonance is almost twice that of the isoscalar resonance; thus one obtains [see Eq. (9)]

$$V_{\text{ad pol}}^{(2)T=1}(r) = +\frac{1}{4} V_{\text{ad pol}}^{(2)T=0}(r). \quad (13)$$

Therefore the added contributions of the  $\lambda=2, T=0$  and  $\lambda=2, T=1$  resonances become

$$V_{\text{ad pol}}^{(2)}(r) = -\frac{5}{4}(0.0208)(A_p^{1/3} + A_T^{1/3}) \times Z_p^2 Z_T^2 / r^6 \text{ (MeV)}. \quad (14)$$

There has been some recent experimental discussion concerning the isoscalar giant octopole resonance.<sup>9</sup> The excitation energy seems to be roughly  $150A^{-1/3}$  MeV. For the purpose of completeness, we give below the polarization potential arising from the coupling to the giant  $3^-$  resonance. It is

$$V_{\text{ad pol}}^{(3)}(r) = -3.56 \times 10^{-3}(A_T + A_p) \times Z_p^2 Z_T^2 / r^8 \text{ (MeV)}. \quad (15)$$

Potentials of higher multiplicities, may also be easily evaluated from our general expression [Eq. (9)]. However, these are of a lesser importance, as the strength of the coupling goes down with  $\lambda$ .

The giant multipole polarization potentials for  $\lambda=1, 2$ , and 3 have been calculated for the systems  $^{16}\text{O} + ^{208}\text{Pb}$  and  $^{208}\text{Pb} + ^{208}\text{Pb}$  at  $E_{\text{c.m.}} = 78$  and 567 MeV, corresponding approximately to their respective Coulomb barrier heights. The results are shown in Fig. 1. Equations (10)–(13) have been used for this purpose. For comparison, we also show in Fig. 1 the ion-ion nuclear interaction constructed from the Christensen-Winther<sup>10</sup> empirical formula,

$$V_n(r) = -50 \frac{R_1 R_2}{R_1 + R_2} \exp\left[-\frac{r - R_1 - R_2}{a_v}\right],$$

with

$$R_i = 1.233A_i^{1/3} - 0.978A_i^{-1/3} \text{ (fm)}$$

and  $a_v = 0.63$  fm.

It is clear from the figure that  $V_{(r)}^{(\lambda)}$  becomes more important than  $V_n(r)$  at distances  $r > 17$  fm. This leads to the conclusion that any unambiguous "observation" of the physical effects generated by  $V_{(r)}^{(\lambda)}$  in the elastic scattering of heavy ions is possible only with energies that correspond to distances of closest approach larger than 17 fm in these cases. This seems to be the case studied by Lynch *et al.*<sup>3</sup> Furthermore, inelastic processes populating discrete states would be sensitive to  $V_{(r)}^{(\lambda)}$  through the form

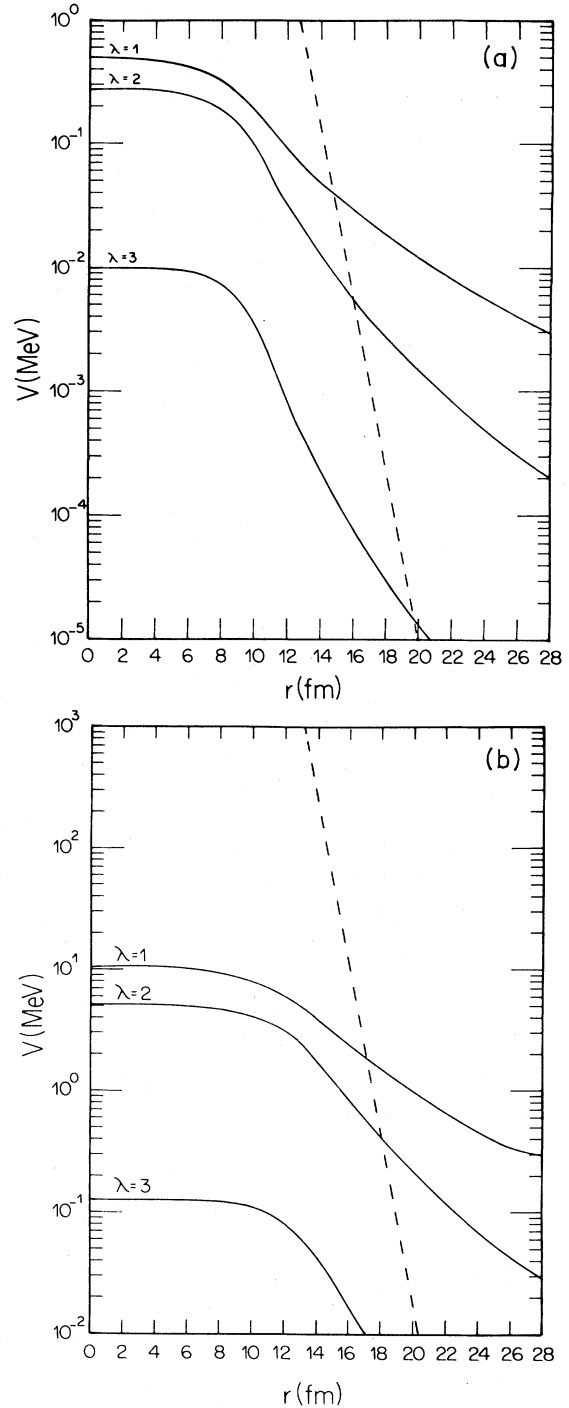


FIG. 1. The giant multipole polarization potentials for  $\lambda=1, 2$ , and 3 for the systems (a)  $^{16}\text{O} + ^{208}\text{Pb}$  and (b)  $^{208}\text{Pb} + ^{208}\text{Pb}$  at  $E_{\text{c.m.}} = 78.0$  and 567.0 MeV, respectively. Also shown is the Christensen-Winther potential.

factor, in the same region where, again,  $V^{(\lambda)} > V_n$ . It would be of interest to further investigate this last point.

Before proceeding to use these potentials, we would like to investigate the quantum mechanical derivation of the adiabatic real potential to see how quantum mechanical

calculations might exhibit the energy and angular momentum independence in the potentials (in contrast to pronounced energy and angular momentum dependence in the nonadiabatic potentials representing real flux loss).

The general form for the nonlocal potential exactly representing the effect of Coulomb excitation on the elastic channel (ignoring reorientation) may be written for a given initial orbital angular momentum  $l$  (Ref. 11)

$$U_l(r, r') = \frac{-2\mu}{k_\lambda \hbar^2} \frac{4\pi}{(2\lambda+1)^2} Z_p^2 e^2 B(E\lambda) \uparrow \sum_{l'} \langle l0\lambda0 | l'0 \rangle^2 \frac{1}{r^{\lambda+1}} \frac{1}{r'^{\lambda+1}} F_{l'}(k_\lambda, r_<) H_{l'}(k_\lambda, r_>), \quad (16)$$

where  $F_{l'}(k_2, r_<)$  and  $H_{l'}(k_2, r_>)$  are regular and outgoing Coulomb wave functions at the momentum  $k_2$  of the excited state. This expression may be written equivalently

$$U_l(r, r') = -\frac{2\mu}{\hbar^2} \frac{8}{(2\lambda+1)^2} Z_p^2 e^2 B(E\lambda) \uparrow \sum_{l'} \langle l0\lambda0 | l'0 \rangle^2 \frac{1}{r^{\lambda+1}} \frac{1}{r'^{\lambda+1}} \int_0^\infty dk \frac{F_{l'}(k, r) F_{l'}(k, r')}{k_\lambda^2 - k^2 + i\epsilon}. \quad (17)$$

Now if the potential is weak in strength its lowest order effect in Born approximation is a source  $\rho(r)$

$$\rho(r) = \int_0^\infty dr' U_l(r, r') F_l(k_0, r'), \quad (18)$$

where  $k_0$  is the ground state momentum. The integral over  $r'$  is then

$$I(k) = \int_0^\infty dr' F_{l'}(k, r') \frac{1}{r'^{\lambda+1}} F_l(k_0, r') \quad (19)$$

and we note that  $I(k)$  is small if  $k = k_2$  and it makes its main contribution when  $k = k_0$ . Thus we ignore the principal part of the integral over  $k$ , factor out the denominator by setting  $k = k_0$ , and obtain

$$U_l(r, r') = -\frac{8}{(2\lambda+1)^2} Z_p^2 e^2 B(E\lambda) \uparrow \sum_{l'} \langle l0\lambda0 | l'0 \rangle^2 \frac{1}{r^{\lambda+1}} \frac{1}{r'^{\lambda+1}} \frac{1}{E_\lambda - E_0} \int_0^\infty dk F_{l'}(k, r) F_{l'}(k, r'). \quad (20)$$

Asymptotically,  $F_l$  becomes a sine function and so the integral over  $k$  is equal to  $(\pi/2)\delta(r - r')$  (Ref. 12) and we can perform the sum over  $l'$  to yield

$$U(r, r') = \frac{-4\pi}{(2\lambda+1)^2} Z_p^2 \frac{e^2 B(E\lambda) \uparrow}{E_\lambda - E_0} \frac{1}{r^{2\lambda+2}} \delta(r - r'), \quad (21)$$

which is equivalent to the local potential [Eq. (5)].

It should be clear that what we have calculated above, Eq. (21), is the contribution to the potential  $U_l(r, r')$  arising from the principal part of the Coulomb Green's function. This part is completely dominant over the contribution arising from the on-energy-shell (imaginary) part of the Coulomb Green's function, when the adiabaticity parameter,  $\xi \equiv \eta_2 - \eta_0 \gg 1$ . Therefore, one may estimate the nonadiabatic contribution to the giant resonance polarization potentials by simply calculating the delta function contribution,

$$\Delta U_l(r, r') = -\frac{2\mu i}{k_\lambda \hbar^2} \frac{4\pi}{(2\lambda+1)^2} Z_p^2 e^2 B(E\lambda) \uparrow \sum_{l'} \langle l0\lambda0 | l'0 \rangle^2 \frac{1}{r^{\lambda+1}} \frac{1}{r'^{\lambda+1}} F_{l'}(k_2 r) F_{l'}(k_\lambda r'). \quad (22)$$

The trivially equivalent local potential is given by

$$\Delta U_l(r, r') = \frac{-\mu i}{2k_\lambda \hbar^2} \frac{4\pi}{(2\lambda+1)^2} Z_p^2 \frac{e^2 B(E\lambda) \uparrow}{a_{02}^\lambda} \sum_{l'} \frac{F_{l'}(k_\lambda r)}{F_l(k_0 r) r^{\lambda+1}} \langle l0\lambda0 | l'0 \rangle I_{l'l_0}^\lambda(\eta_0, \eta_2), \quad (23)$$

where  $a_{02}$  is the symmetrized half distance of closest approach for a head-on collision, and  $I_{l'l_0}^\lambda(\eta_2, \eta_0)$  is the Coulomb excitation radial matrix element. This matrix element approaches the classical orbital integral  $I_{\lambda\mu}(\theta, \xi)^2$ ,  $\mu \equiv l - l'$ , in the limit  $\eta_0 \eta_2 \gg 1$ , which is certainly attained at sub-barrier energies. In the limit  $(\xi/\sin\theta/2) \gg 1$ ,  $I_{\lambda\mu}(\theta, \xi)$  may be approximated by the expression<sup>2</sup>

$$I_{\lambda\mu}(\theta, \xi) = \frac{2\pi}{\Gamma[\frac{1}{2}(\lambda - \mu + 1)]} \exp \left[ -\xi \left( \frac{1}{\sin\theta/2} + \frac{\pi}{2} \right) \right] \times \xi^{(\lambda - \mu - 1)/2} \left( \frac{1}{2} \sin\theta/2 \right)^{\frac{\lambda + \mu + 1}{2}}, \quad (24)$$

which clearly shows that in the back-angle region  $I_{\lambda\mu}$  is

very small, thus rendering  $\Delta U_l^{(\lambda)}(r)$  insignificant.

Our expression for  $\Delta U_l^{(\lambda)}(r)$ , Eq. (22), is not very useful, as it involves the ratio

$$\frac{F_{l'}(k_\lambda, r)}{F_l(k, r)}.$$

However, the effect of  $\Delta U$  on the wave function may be estimated easily to be

$$\Delta \psi \simeq -\frac{2\mu i}{k_\lambda \hbar^2} \frac{4\pi}{(2\lambda+1)^2} Z_p^2 \frac{e^2 B(E\lambda) \uparrow}{a_{02}^{2\lambda}} \times \sum \langle l0\lambda0 | l'0 \rangle^2 [I_{l'l_0}^\lambda(\eta_0, \eta_\lambda)]^2, \quad (25)$$

which goes approximately as  $e^{-3\xi}$  at  $\theta = 180^\circ$ .

### III. EFFECTS OF RELATIVITY

We consider Coulomb elastic scattering of a spin zero projectile on a spin zero target. A classical Hamiltonian may be written which contains relativistic effects to first order in  $1/mc^2$ . This Darwin Hamiltonian<sup>18</sup> takes the following form in the center of mass system

$$H = \frac{p^2(m_1+m_2)}{2m_1m_2} + \frac{Z_1Z_2e^2}{r} - \frac{p^4}{8c^2} \left( \frac{1}{m_1^3} + \frac{1}{m_2^3} \right) + \frac{Z_1Z_2e^2}{2m_1m_2c^2} \left( \frac{p^2+p_r^2}{r} \right). \quad (26)$$

The first two terms on the right-hand side are the usual nonrelativistic forms. The third term arises from the momentum correction of special relativity. The fourth term comes from the magnetic interaction arising from the motion of a finite mass target.

To evaluate the effect of these last two terms we begin by rewriting the radial momentum  $p_r$

$$p_r^2 = p^2 - \frac{L^2}{r^2}, \quad (27)$$

where  $L$  is the orbital angular momentum of the scattering system. Furthermore, only in these correction terms do we make use of the zeroth order expression for  $p^2$

$$p^2 = \frac{2m_1m_2}{(m_1+m_2)} \left[ E - \frac{Z_1Z_2e^2}{r} \right], \quad (28)$$

where  $E$  is the asymptotic center of mass kinetic energy.

If one makes these substitutions and collects terms, the Hamiltonian becomes

$$H = \frac{p^2(m_1+m_2)}{2m_1m_2} - \frac{(m_1^2+m_2^2-m_1m_2)}{2(m_1+m_2)m_1m_2c^2} E^2 + \frac{Z_1Z_2e^2}{r} \left[ 1 + \frac{(m_1^2+m_2^2+m_1m_2)E}{(m_1+m_2)m_1m_2c^2} \right] - \frac{(m_1^2+m_2^2+3m_1m_2)}{2(m_1+m_2)m_1m_2c^2} \left( \frac{Z_1Z_2e^2}{r} \right)^2 - \frac{Z_1Z_2e^2}{2m_1m_2c^2} \frac{L^2}{r^3}. \quad (29)$$

The effects of the last two terms (in  $1/r^2$  and  $L^2/r^3$ ) will be calculated by classical perturbation theory in Sec. IV. We will ignore the relativistic effects in the slight change of constants in the other terms which give a slight angle-independent change in the overall cross section equivalent to a slight change in the beam energy.

### IV. EVALUATION OF THE CROSS SECTION

In this section, we derive closed expressions for the cross section of heavy ion elastic scattering in the combined Coulomb plus giant multipole polarization potentials and "relativistic" potential discussed in Sec. III. Since the Sommerfeld parameter of the heavy-ion (HI) system at sub-barrier energies is quite large, we are al-

lowed to use classical scattering theory. The exact form of the criterion for the applicability of classical description of scattering was considered by Bohr<sup>13</sup> and is given by

$$\left| \lambda \frac{\partial \theta(b)}{\partial b} \right| \ll \theta(b), \quad (30)$$

where  $\lambda$  is the de Broglie wavelength of relative motion, and  $\theta(b)$  is the classical deflection function. Thus as long as the deflection function does not exhibit rapid variation with the impact parameter  $b$ , classical mechanics is adequate. In our case  $\theta(b)$  is different from the Rutherford deflection function

$$\theta_{\text{Ruth}}(b) = 2 \tan^{-1} \frac{\eta}{kb},$$

a slowly varying function of  $b$ , by a very small deviation which, as we show below, is also slowly varying with  $b$ . Accordingly we are quite justified in using classical scattering theory to calculate  $d\sigma/d\Omega$ . Furthermore, since the effect of the polarization potentials is rather small, we calculate their effect using first order classical perturbation theory. Namely, writing for the deflection function

$$\theta(b) = \theta_{\text{Ruth}}(b) + \Delta\theta^{(\lambda)}(b), \quad (31)$$

$\Delta\theta^{(\lambda)}$  is given by<sup>14</sup>

$$\Delta\theta^{(\lambda)} = -\frac{1}{E} \frac{\partial}{\partial b} \left[ \frac{1}{b} \int_0^{\phi_0} r^2 V_{\text{ad pol}}^{(\lambda)}(r) d\phi \right],$$

where  $\phi_0$  is defined by

$$\phi_0 = \frac{\pi - \theta}{2}. \quad (32)$$

The variable angle  $\phi$ , which is depicted in Fig. 2 defines the trajectory equation for Coulomb scattering

$$\frac{1}{r} = \frac{1}{a} \frac{\cos\phi_0}{\sin^2\phi_0} (\cos\phi - \cos\phi_0),$$

where  $a = \eta/k = (Z_1Z_2e^2)/2E$ , half the distance of closest approach for a head-on collision.

The classical cross section,

$$\frac{d\sigma}{d\Omega} = \frac{b}{\sin\theta} \left| \frac{db}{d\theta} \right|$$

attains the following form when  $\Delta\theta^{(\lambda)}$  is included to first order:

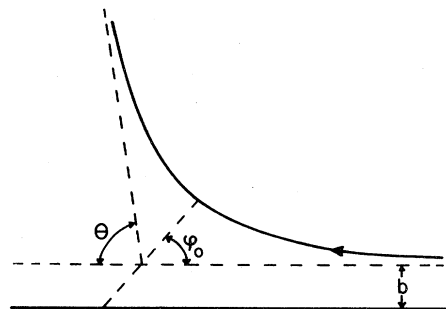


FIG. 2. The Coulomb scattering variables [see Eq. (32)].

$$\frac{d\sigma}{d\Omega} = \frac{d\sigma_{\text{Ruth}}}{d\Omega} \left[ 1 + \frac{1}{2} \Delta\theta^{(\lambda)} \tan \frac{\theta}{2} + \frac{3}{2} \Delta\theta^{(\lambda)} \cot \frac{\theta}{2} + \frac{1}{2} \frac{d}{d\phi_0} \Delta\theta^{(\lambda)} \right]. \quad (33)$$

At  $\theta = \pi$ ,  $\phi_0 = 0$ , and  $\Delta\theta^{(\lambda)} = 0$ . Therefore, the value of the

cross section at  $\theta = \pi$  is

$$\frac{d\sigma}{d\Omega}(\lambda) = \frac{d\sigma_{\text{Ruth}}}{d\Omega}(\pi) \left[ 1 + \frac{d}{d\phi_0} \Delta\theta^{(\lambda)}(\pi) \right]. \quad (34)$$

We now apply our formulae given above for  $\lambda = 1, 2$ , and  $3$ , obtaining,

$$\Delta\theta^{(1)} = -\frac{V_0^{(1)}}{2Ea^4} \frac{\cos^4 \phi_0}{\sin^6 \phi_0} (-15\phi_0 + 12\phi_0 \sin^2 \phi_0 + 15 \sin \phi_0 \cos \phi_0 - 2 \cos \phi_0 \sin^3 \phi_0), \quad (35)$$

$$\Delta\theta^{(2)} = -\frac{V_0^{(2)}}{8Ea^6} \frac{\cos^6 \phi_0}{\sin^{10} \phi_0} (-315\phi_0 + 420\phi_0 \sin^2 \phi_0 - 120\phi_0 \sin^4 \phi_0 + 315 \cos \phi_0 \sin \phi_0 - 210 \cos \phi_0 \sin^3 \phi_0 + 8 \cos \phi_0 \sin^5 \phi_0), \quad (36)$$

$$\Delta\theta^{(3)} = -\frac{V_0^{(3)}}{80Ea^8} \frac{\cos^8 \phi_0}{\sin^{14} \phi_0} (-15015\phi_0 + 27720\phi_0 \sin^2 \phi_0 - 15120\phi_0 \sin^4 \phi_0 + 2240\phi_0 \sin^6 \phi_0 + 15015 \sin \phi_0 \cos \phi_0 - 17710 \cos \phi_0 \sin^3 \phi_0 + 4648 \cos \phi_0 \sin^5 \phi_0 - 80 \cos \phi_0 \sin^7 \phi_0). \quad (37)$$

As shown in Fig. 3, the three angular deviations have similar behavior, all peaking at an intermediate angle. Furthermore, they attain zero value at  $\phi_0 = 0$  and  $\pi/2$  which correspond to  $\theta = 0$  and  $\pi$ , respectively, see Eq. (32).

When inserted in Eq. (33) for the cross section, Eqs. (35)–(37) give the following expressions:

$$\frac{d\sigma^{(1)}}{d\Omega} = \frac{d\sigma_{\text{Ruth}}}{d\Omega} \left\{ 1 - \frac{V_0^{(1)}}{2Ea^4} \frac{\cos^3 \phi_0}{\sin^7 \phi_0} \left[ \frac{3}{2} (1 + 16 \cos^2 \phi_0 + 8 \cos^4 \phi_0) - \frac{1}{2} (29 + 46 \cos^2 \phi_0) \cos \phi_0 \sin \phi_0 \right] \right\}, \quad (38)$$

$$\frac{d\sigma^{(2)}}{d\Omega} = \frac{d\sigma_{\text{Ruth}}}{d\Omega} \left\{ 1 - \frac{V_0^{(2)}}{8Ea^6} \frac{\cos^6 \phi_0}{\sin^{10} \phi_0} \left[ \left( -\frac{3}{2} \tan \phi_0 - \frac{9}{2} \cot \phi_0 \right) (-315\phi_0 + 420\phi_0 \sin^2 \phi_0 - 120\phi_0 \sin^4 \phi_0 - 315 \cos \phi_0 \sin \phi_0 - 210 \cos \phi_0 \sin^3 \phi_0 + 8 \cos \phi_0 \sin^5 \phi_0) + \frac{1}{2} (840\phi_0 \sin \phi_0 \cos \phi_0 - 480\phi_0 \sin^3 \phi_0 \cos \phi_0 - 840 \sin^2 \phi_0 + 960 \sin^4 \phi_0 - 48 \sin^6 \phi_0) \right] \right\}, \quad (39)$$

and

$$\frac{d\sigma^{(3)}}{d\Omega} = \frac{d\sigma_{\text{Ruth}}}{d\Omega} \left\{ 1 - \frac{V_0^{(3)}}{80Ea^8} \frac{\cos^8 \phi_0}{\sin^{14} \phi_0} \left[ \left( -\frac{5}{2} \tan \phi_0 - \frac{13}{2} \cot \phi_0 \right) (-15015\phi_0 + 27720\phi_0 \sin^2 \phi_0 - 15120\phi_0 \sin^4 \phi_0 + 2240\phi_0 \sin^6 \phi_0 + 15015 \cos \phi_0 \sin \phi_0 - 17710 \cos \phi_0 \sin^3 \phi_0 + 4648 \cos \phi_0 \sin^5 \phi_0 - 80 \cos \phi_0 \sin^7 \phi_0) + \frac{1}{2} (55440\phi_0 \cos \phi_0 \sin \phi_0 - 60480\phi_0 \cos \phi_0 \sin^3 \phi_0 + 13440\phi_0 \cos \phi_0 \sin^5 \phi_0 - 55440 \sin^2 \phi_0 + 78960 \sin^4 \phi_0 - 26208 \sin^6 \phi_0 + 640 \sin^8 \phi_0) \right] \right\}. \quad (40)$$

We write the percentage deviation

$$\Delta\sigma^{(\lambda)} \equiv \left[ \frac{d\sigma^{(\lambda)}}{d\Omega} - \frac{d\sigma_{\text{Ruth}}}{d\Omega} \right] / \frac{d\sigma_{\text{Ruth}}}{d\Omega}$$

in the following form:

$$\Delta\sigma^{(1)} = -\frac{V_0^{(1)}}{2Ea^4} g^{(1)}(\theta),$$

$$\Delta\sigma^{(2)} = -\frac{V_0^{(2)}}{8Ea^6} g^{(2)}(\theta), \quad (41)$$

$$\Delta\sigma^{(3)} = -\frac{V_0^{(3)}}{80Ea^8} g^{(3)}(\theta).$$

The three universal functions  $g^{(1)}(\theta)$ ,  $g^{(2)}(\theta)$ , and  $g^{(3)}(\theta)$  are shown in Fig. 4. As one clearly sees, all universal functions attain their maximum value at  $\theta = 180^\circ$ . Furthermore, they have zero contribution at  $\theta = 0$ . Thus measurement of these effects in the backward hemisphere should be compared with forward scattering at each energy. We should mention that Eq. (38) for  $\lambda = 1$  has been previously obtained by Baur *et al.*<sup>4</sup> A simple measure of

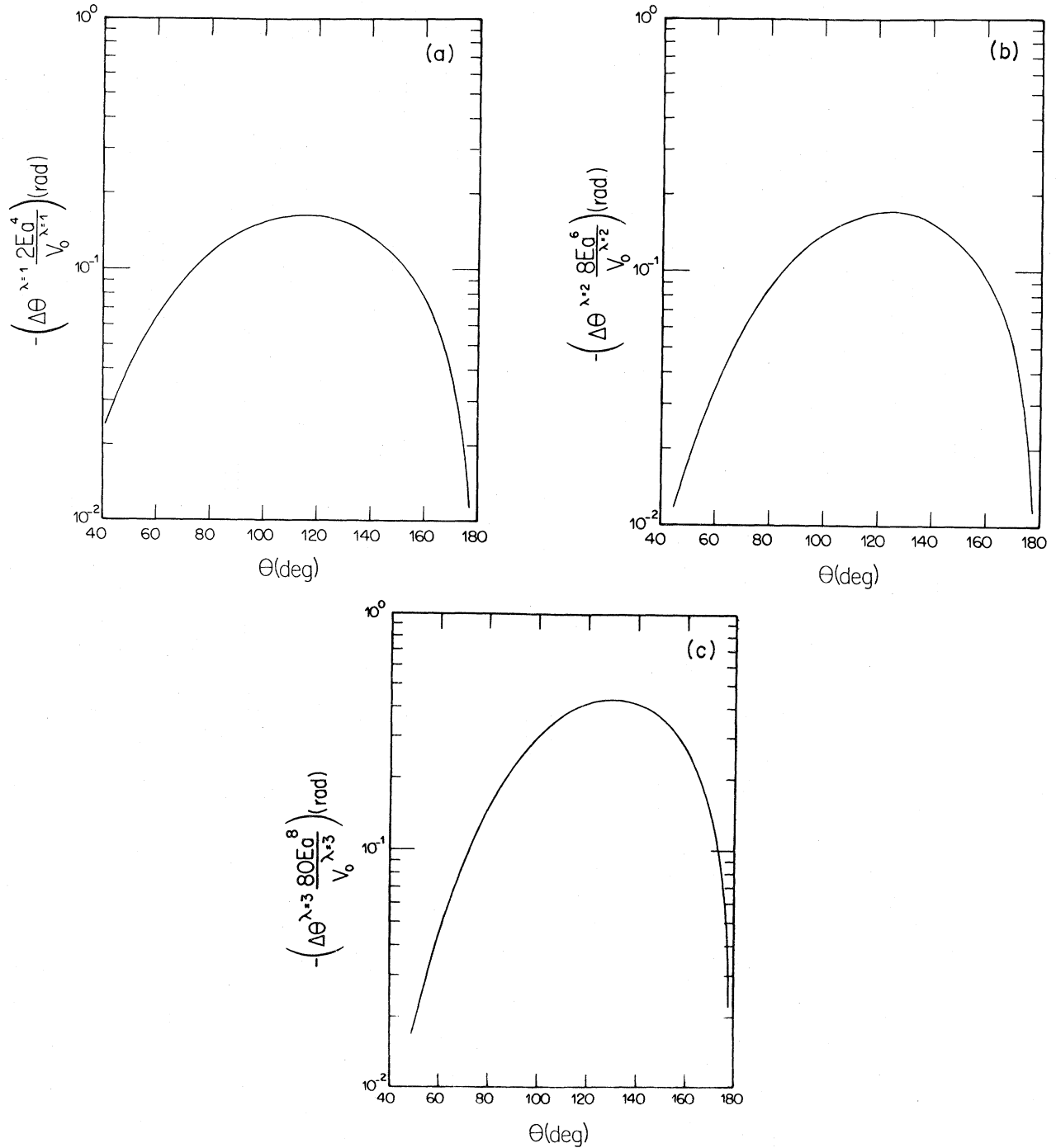


FIG. 3. The angular deviations,  $\Delta\theta^{\lambda=1}$ ,  $\Delta\theta^{\lambda=2}$ , and  $\Delta\theta^{\lambda=3}$ , plotted versus the center of mass angles.

$\Delta\sigma^{(\lambda)}$  may be obtained by setting  $\theta=180^\circ$ . After tedious calculation we find

$$\begin{aligned} \Delta\sigma^{(1)}(\theta=\pi) &= \frac{3.66E^3}{(Z_1Z_2e^2)^4} V_0^{(1)}, \\ \Delta\sigma^{(2)}(\theta=\pi) &= \frac{4.43E^5}{(Z_1Z_2e^2)^6} V_0^{(2)}, \\ \Delta\sigma^{(3)}(\theta=\pi) &= \frac{5.09E^7}{(Z_1Z_2e^2)^8} V_0^{(3)}. \end{aligned} \quad (42)$$

Note that  $V_0^{(\lambda)}$  is intrinsically negative.

Since the numerical factors appearing in the expressions above vary very slowly with  $\lambda$ , one may, to get an order of magnitude estimate of  $\Delta\sigma^{(\lambda)}$ , write a general expression valid for any  $\lambda$

$$\Delta\sigma^{(\lambda)}(\theta=\pi) \simeq \frac{E^{2\lambda+1}}{(Z_1Z_2e^2)^{2\lambda+2}} V_0^{(\lambda)}, \quad (43)$$

with  $V_0^{(\lambda)}$  given by  $r^{2\lambda+2} V_{\text{ad pol}}^{(\lambda)}(r)$  [see Eq. (9)].

The calculation of the deviation  $\Delta\sigma^{(R)}$  due to relativis-

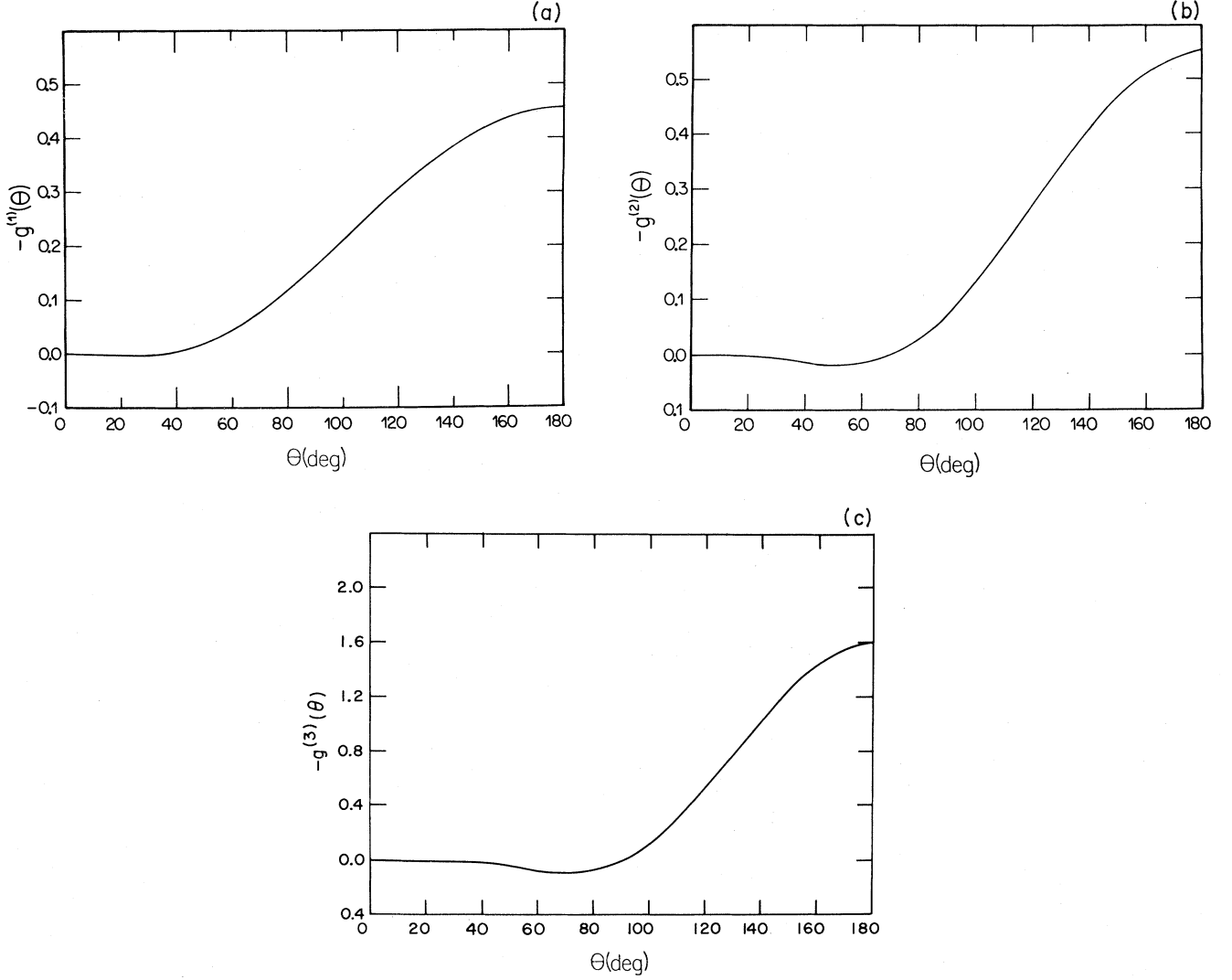


FIG. 4. The universal functions  $g^{(1)}(\theta)$ ,  $g^{(2)}(\theta)$ , and  $g^{(3)}(\theta)$ , Eq. (41), plotted versus the center of mass angle.

tic effects is straightforward and follows the same lines as the ones used to evaluate  $\Delta\sigma^{(\lambda)}$  above. As we have seen in Sec. III, there are two "polarization" terms arising from special relativity [Eq. (29)], namely

$$V_1^{(R)} = -\frac{m_1^2 + m_2^2 + 3m_1m_2}{2(m_1 + m_2)m_1m_2c^2} \left[ \frac{Z_1Z_2e^2}{r} \right]^2, \quad (44)$$

$$V_2^{(R)} = -\frac{Z_1Z_2e^2}{2m_1m_2c^2} \frac{L^2}{r^3}. \quad (45)$$

The corresponding changes in the classical deflection function, Eqs. (31) and (32), may be easily evaluated

$$\Delta\theta_1^{(R)} = \frac{m_1^2 + m_2^2 + 3m_1m_2}{2(m_1 + m_2)m_1m_2c^2} \frac{(Z_1Z_2e^2)^2}{Ea^2} \cot^2\phi_0 \times (-\phi_0 + \sin\phi_0\cos\phi_0), \quad (46)$$

$$\Delta\theta_2^{(R)} = -\frac{Z_1Z_2e^2}{2m_1m_2c^2} \frac{2m_1m_2}{(m_1 + m_2)a} \cot^2\phi_0 \times (-\phi_0 + \sin\phi_0\cos\phi_0). \quad (47)$$

Summing, Eqs. (46) and (47), and noting that the classical distance of closest approach  $2a$  is equal to  $(Z_1Z_2e^2)/E$ , we obtain the total change in the deflection function due to relativistic effects

$$\Delta\theta^{(R)} = \frac{2E}{\mu c^2} \cot^2\phi_0 (-\phi_0 + \frac{1}{2}\sin^2\phi_0), \quad (48)$$

where  $\mu = m_1m_2/(m_1 + m_2)$ , is the reduced mass. The effect on the Rutherford cross section then obtains from Eq. (33)

$$\frac{d\sigma^{(R)}}{d\Omega} = \frac{d\sigma_{\text{Ruth}}}{d\Omega} \left\{ 1 + \frac{2E}{\mu c^2} \tan^2\frac{\theta}{2} \left[ \frac{1}{2} \cot\theta(\sin\theta + \theta - \pi) - \cos^2\frac{\theta}{2} \right] \right\}. \quad (49)$$



The corresponding universal angle-function  $g^{(R)}(\theta)$  defined through

$$\Delta\sigma^{(R)} = -\frac{2E}{\mu c^2} g^{(R)}(\theta) \quad (50)$$

is shown in Fig. 5.

Note that in Eq. (49) there is no dependence on  $Z_1 Z_2$  in the relativistic correction term; factors of  $Z_1 Z_2$  in the potential have been canceled by the  $Z_1 Z_2$  implicit in the  $a$  from the classical trajectory. At  $180^\circ$  the angle dependent coefficient of  $2E_{c.m.}/\mu c^2$  is  $-\frac{2}{3}$ , and it remains negative going to  $-\frac{1}{2}$  at  $90^\circ$  and to  $-\pi\theta/8$  at small angles. For an infinite mass target  $\mu$  is equal to the projectile mass, and  $2E_{c.m.}/\mu c^2$  is equal to  $V_\infty^2/c^2$ . For a finite mass target relativistic magnetic effects enter in, and their lowest order effect in combination with the lowest order relativistic scalar potential term is to cause the mass,  $\mu$  in Eq. (49) to be equal to the reduced mass of the system. For the case of spin  $\frac{1}{2}$  electron scattering a similar relativistic correction has been derived to lowest order in  $Z_1 Z_2 e^2/\hbar c$  (which is inappropriate here), but it only includes the  $\cos^2\theta/2$  term in the square brackets.<sup>15</sup>

We present in Table I the results obtained from Eq. (42) for several heavy-ion systems with  $E$  taken to be equal to the height of the Coulomb barrier at  $1.44(A_p^{1/3} + A_T^{1/3})$  fm. The strengths  $V_0^{(\lambda)}$  are calculated from Eqs. (8) and (9). The effect on the cross section is as large as 2% for the summed effect of dipole, quadrupole, and octopole excitations with two heavy nuclei and about 0.6% for  $^{16}\text{O}$  on a heavy nucleus. Though the octopole excitation is quite small, the quadrupole one is not negligible, a little less than half that of the dipole. The relativistic effect is largest for uranium on uranium (0.8%), but not much less for any of the other cases.

Since the experiments of Lynch *et al.*<sup>3</sup> were done at very low energies, the dipole effect (which goes as  $E^3$ ) is relatively more important than the quadrupole effect (which goes as  $E^5$ ) when compared to our calculation of 78 MeV  $^{16}\text{O}$  on  $^{208}\text{Pb}$ . The highest energy measured was 55.7 MeV which corresponds to a distance of closest approach,  $2.0(A_p^{1/3} + A_T^{1/3})$  fm. At this energy we calculate quadrupole contribution of  $\Delta\sigma^{(2)} = -0.03\%$  at  $150^\circ$ , to be added to the dipole contribution of  $-0.2\%$  obtained by these authors with a  $V_0^{(1)} = -2.24 \times 10^3$  (MeV fm), slightly larger in magnitude than our  $V_0^{(1)}$  value. Our formula for  $\Delta\sigma^{(R)}$  agrees with the angular curve for 50 MeV

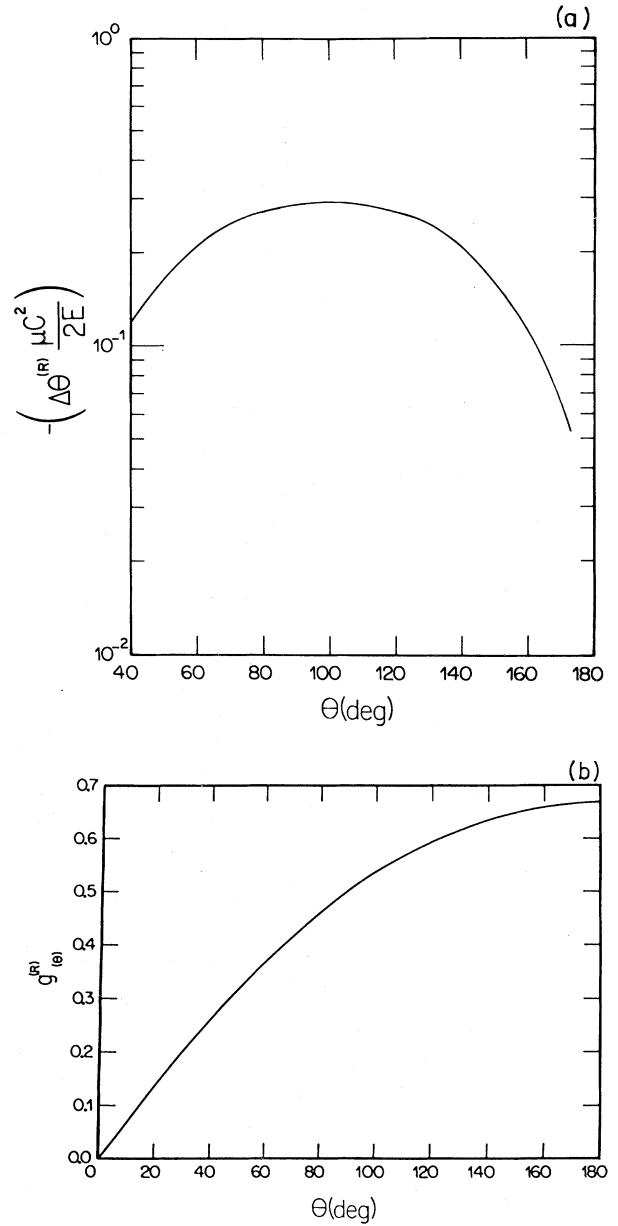


FIG. 5. The universal function  $g^{(R)}(\theta)$  associated with the relativistic effects, Eq. (50), plotted versus the center of mass angle.

TABLE I. Adiabatic polarization potentials due to giant dipole, quadrupole, and octopole excitations are tabulated. Percentage reduction in  $180^\circ$  cross sections are also shown for each contribution as well as for the relativistic effects. Reductions are angular, relative only to the  $(\sin\theta/2)^{-4}$  Rutherford distribution.

System	$E_{c.m.}$ (MeV)	$V_0^{(1)}$ (MeV fm <sup>4</sup> )	$V_0^{(2)}$ (MeV fm <sup>6</sup> )	$V_0^{(3)}$ (MeV fm <sup>8</sup> )	$V_0^{(R)}$	$\Delta\sigma^{(1)}$ (%)	$\Delta\sigma^{(2)}$ (%)	$\Delta\sigma^{(3)}$ (%)	$\Delta\sigma^{(R)}$ (%)
$^{40}\text{Ar} + ^{160}\text{Gd}$	130	$6.24 \times 10^3$	$3.05 \times 10^5$	$9.45 \times 10^5$	$8.73 \times 10^{-3}$	0.66	0.24	$5.26 \times 10^{-3}$	0.582
$^{40}\text{Ar} + ^{148}\text{Sm}$	128	$5.71 \times 10^3$	$2.81 \times 10^5$	$8.34 \times 10^5$	$8.74 \times 10^{-3}$	0.66	0.24	$5.37 \times 10^{-3}$	0.583
$^{16}\text{O} + ^{148}\text{Sm}$	64	$1.08 \times 10^3$	$4.99 \times 10^4$	$1.44 \times 10^5$	$9.52 \times 10^{-3}$	0.40	0.176	$4.76 \times 10^{-3}$	0.635
$^{16}\text{O} + ^{208}\text{Pb}$	78	$1.89 \times 10^3$	$9.45 \times 10^4$	$3.43 \times 10^5$	$1.13 \times 10^{-2}$	0.42	0.168	$4.84 \times 10^{-3}$	0.753
$^{208}\text{Pb} + ^{208}\text{Pb}$	567	$1.57 \times 10^5$	$1.39 \times 10^7$	$6.70 \times 10^7$	$1.17 \times 10^{-2}$	1.192	0.44	$8.32 \times 10^{-3}$	0.780
$^{238}\text{U} + ^{238}\text{U}$	683	$2.45 \times 10^5$	$2.30 \times 10^7$	$1.21 \times 10^8$	$1.23 \times 10^{-2}$	1.30	0.46	$8.77 \times 10^{-3}$	0.820

$^{16}\text{O} + ^{208}\text{Pb}$  calculated numerically by Lynch *et al.*,<sup>3</sup> and we also agree with their energy dependent calculation of the relativistic effect.

### V. COMPARISON WITH COUPLED CHANNELS CALCULATION AND TRIVIAALLY EQUIVALENT LOCAL POTENTIAL

To investigate the validity of our classical calculation reported above we have performed several computer calculations for the quadrupole case. We take as our test case the isoscalar quadrupole giant resonance in  $^{208}\text{Pb}$  excited by 78 MeV (c.m.)  $^{16}\text{O}$ . The sum rule gives us  $B(E2)$  of  $8055 e^2 \text{ fm}^4$  which with  $E_x = 10.13$  MeV corresponds to a polarization potential of  $-53035/r^6$  MeV.

Figure 6 shows an angular distribution of the ratio to Rutherford cross section from an analytical formula [Eq. (24)]. Also on the same figure are the results of an optical model code evaluation of the cross section with the potential  $-53035/r^6$  and also results of a Coulomb excitation coupled channels calculation with no potential but with quadrupole coupling to the 10.13 MeV state with the above  $B(E2)$  strength. All three calculations agree to within about a percent of the deviation from Rutherford scattering at all angles. This not only ensures us that the classical scattering theory provides a very accurate cross section for the  $1/r^6$  potential, but that the adiabatic polarization potential truly and accurately represents the effects of channel coupling when used to provide a cross section calculation.

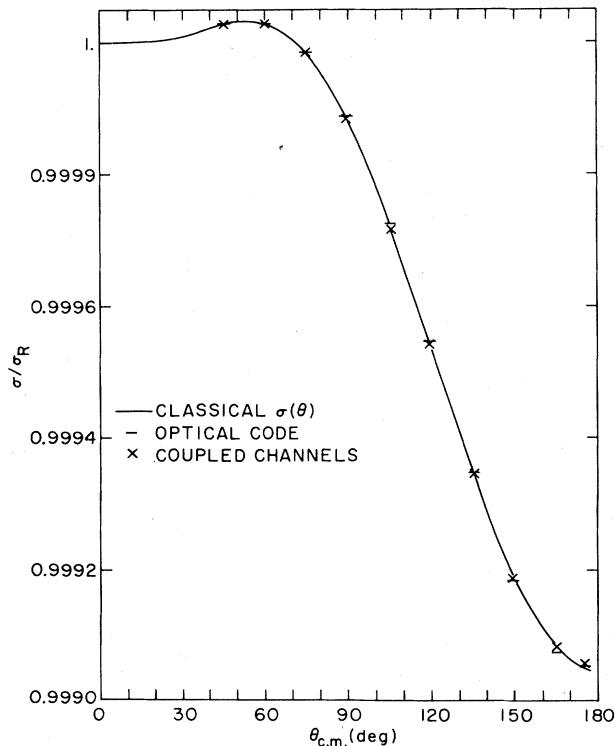


FIG. 6. Cross sections as ratio to Rutherford for 78 MeV (c.m.)  $^{16}\text{O} + ^{208}\text{Pb}$  with parameters in the text. Optical model and coupled channels calculations were performed with the code CHORK.<sup>17</sup>

It is interesting to consider the potential further. If one has solved a set of coupled Schrödinger equations for a given partial wave, then one may define a trivially equivalent local potential (TELP) to represent the effect of the off-diagonal coupling upon the elastic channel

$$\left[ \frac{d^2}{dr^2} + k_0^2 - \frac{l_0(l_0+1)}{r^2} - \frac{2\mu}{\hbar^2} V_0(r) \right] X_{l_0}(r) = \sum_j V_{0j}(r) X_j(r) \equiv \frac{2\mu_0}{\hbar^2} V_{\text{TELP}}(r) X_{l_0}(r), \quad (51)$$

where  $X_{l_0}(r)$  is the full solution of the coupled channels problem, not just the homogeneous part.

Figure 7 shows the results of computing the  $V_{\text{TELP}}$  for three initial orbital angular momenta in our test case compared with the analytical  $1/r^6$  potential in the crucial turning point region for each partial wave. As one moves out from the turning point one sees the "hair" seen in optical potentials previously calculated<sup>11,16</sup> in the "sudden" case of coupling to low lying states. An exploratory calculation at a lower energy [64 MeV (c.m.)] verifies that  $V_{\text{TELP}}$  is also energy independent in the sense that the values of  $V_{\text{TELP}}$  always approximated the energy independent  $1/r^6$  potential in the turning point regions.

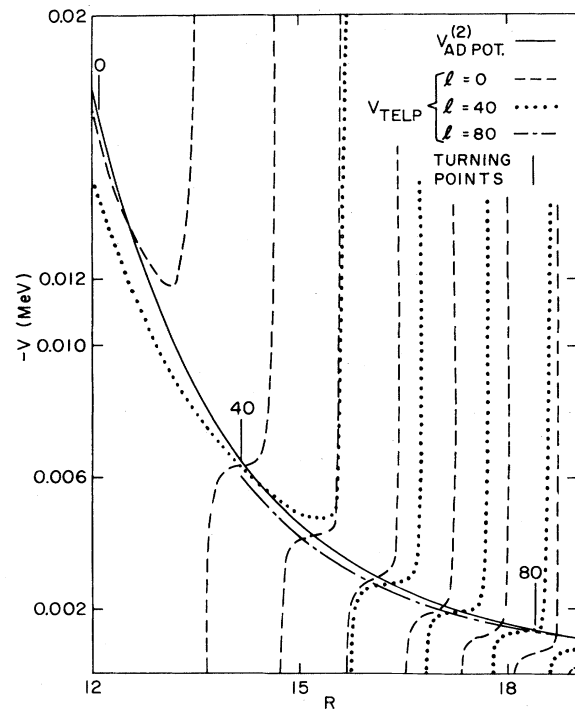


FIG. 7. Comparison of trivially equivalent potential computed with the code CHORK (Ref. 17) for orbital angular momenta 0, 40, and 80 with the analytical form. Parameters are the same as for Fig. 1 (see the text).

## VI. CONCLUSION

In this paper we have presented a detailed discussion of the small deviations, in the sub-barrier elastic scattering of heavy ions, that arise from virtual giant resonance excitation and relativistic correction. We have found that these effects manifest themselves unambiguously at center of mass energies corresponding to Coulomb distances of closest approach larger than about 17 fm in the cases considered.

Using a perturbative classical scattering calculation, we have assessed the importance of these polarization potentials in the elastic scattering cross section. We have found that it is more than sufficient to consider the dipole and quadrupole together with the relativistic correction potentials in considering the 1% deviation from pure Ruther-

ford scattering.

Our classical calculation of the giant quadrupole polarization effect on the cross section has been compared with exact coupled channels calculations and with an optical model code evaluation of the  $1/r^6$  potential. Agreement was excellent, from which one may infer that not only is the  $1/r^{2\lambda+2}$  potential an excellent representation of virtual excitation, but that the classical scattering theory is an excellent representation of the effect of these potentials.

This work was supported in part by the Conselho Nacional de Pesquisas (CNPq)-Brasil, by Fundação de Amparo à Pesquisa do Estado de São Paulo (FAPESP)-Brasil, and by the U. S. Department of Energy Contract DE-AC02-76CH00016.

- 
- <sup>1</sup>C. E. Thorn, M. J. Levine, J. J. Kolata, C. Flaum, P. D. Bond, and J. C. Sens, *Phys. Rev. Lett.* **38**, 384 (1977); P. Doll, M. Bini, D. L. Hendrie, J. Mahoney, A. Menehaca-Rocha, D. K. Scott, T. J. M. Symons, K. van Bibber, Y. P. Viyogi, H. Wieman, and A. J. Baltz, *Phys. Lett.* **76B**, 566 (1978).
- <sup>2</sup>K. Alder, and A. Winther, *Electromagnetic Excitation* (North-Holland, Amsterdam, 1975).
- <sup>3</sup>W. G. Lynch, M. B. Tsang, H. C. Bhang, J. G. Cramer, and R. J. Puigh, *Phys. Rev. Lett.* **48**, 979 (1982).
- <sup>4</sup>G. Baur, F. Rösler, and D. Trautmann, *Nucl. Phys.* **A288**, 113 (1977).
- <sup>5</sup>A. J. Baltz and M. S. Hussein, *Phys. Lett.* **132B**, 274 (1983).
- <sup>6</sup>K. Alder, A. Bohr, T. Huus, B. R. Mottelson, and A. Winther, *Rev. Mod. Phys.* **28**, 432 (1956).
- <sup>7</sup>A. Bohr and B. R. Mottelson, *Nuclear Structure* (Benjamin, New York, 1975), Vol. II.
- <sup>8</sup>J. Rasmussen, P. Möller, M. Guidry, and R. Neese, *Nucl. Phys.* **A341**, 149 (1980); M. S. Hussein, Proceedings of the 1st Brazilian Symposium on Photo-Nuclear Reactions, São Paulo, 1982 (unpublished).
- <sup>9</sup>R. Bonin, N. Alamanos, B. Berthier, G. Bruge, J. L. Escudie, H. Faraggi, D. Legrand, J. C. Lugol, W. Mittig, L. Papineau, J. Arvieux, L. Farvacque, M. Levine, D. K. Scott, A. I. Yavin, and M. Buenerd, Michigan State University annual report, 1982, p. 50.
- <sup>10</sup>P. R. Christensen and A. Winther, *Phys. Lett.* **65B**, 19 (1976).
- <sup>11</sup>A. J. Baltz, S. K. Kauffmann, N. K. Glendenning, and K. Pruess, *Phys. Rev. Lett.* **40** 20 (1978); *Nucl. Phys.* **A327**, 221 (1979); B. V. Carlson, M. S. Hussein, and A. J. Baltz, *Phys. Lett.* **98B**, 409 (1981); *Ann. Phys. (N.Y.)* **138**, 215 (1982).
- <sup>12</sup>L. I. Schiff *Quantum Mechanics* (McGraw-Hill, New York, 1955).
- <sup>13</sup>N. Bohr, *K. Dans. Vidensk. Selsk. Mat. Fys. Medd.* XVIII, no. 8 (1948); M. S. Hussein, Y. T. Chen, and F. I. A. Almeida, *Am. J. Phys.* (in press).
- <sup>14</sup>L. D. Landau and E. M. Lifshitz, *Mechanics* (Pergamon, London, 1960).
- <sup>15</sup>N. J. Mott and H. S. W. Massey, *The Theory of Atomic Collisions*, 3rd ed. (Clarendon, Oxford, 1965).
- <sup>16</sup>M. A. Franey and P. J. Ellis, *Phys. Rev. C* **23** 787 (1981).
- <sup>17</sup>CHORK: version of coupled channels code CHUCK by P. D. Kunz as modified by L. Rickertson (unpublished).
- <sup>18</sup>J. D. Jackson, *Classical Electrodynamics*, 2nd ed. (Wiley, New York, 1975), p. 616.